

# Event2Vec: Processing neuromorphic events directly by representations in vector space

Wei Fang<sup>1</sup> and Priyadarshini Panda<sup>1</sup>

<sup>1</sup>Electrical & Computer Engineering, Yale University.

Contributing authors: [wei.fang@yale.edu](mailto:wei.fang@yale.edu); [priya.panda@yale.edu](mailto:priya.panda@yale.edu);

## Abstract

The neuromorphic event cameras have overwhelming advantages in temporal resolution, power efficiency, and dynamic range compared to traditional cameras. However, the event cameras output asynchronous, sparse, and irregular events, which are not compatible with mainstream computer vision and deep learning methods. Various methods have been proposed to solve this issue, but at the cost of long preprocessing procedures, losing temporal resolutions, or being incompatible with massively parallel computation. Inspired by the great success of the word to vector, we summarize the similarities between words and events, then propose the first event to vector (event2vec) representation. We validate event2vec on classifying the DVS Gesture and ASL-DVS dataset, showing impressive learning efficiency and accuracy. Beyond task performance, the most attractive advantage of event2vec is that it aligns events to the domain of natural language processing, showing the promising prospect of integrating events into large language and multimodal models. Our codes, models, and training logs are available at <https://github.com/fangwei123456/event2vec>.

**Keywords:** neuromorphic computing, event-based vision, brain-inspired computing

## 1 Introduction

Neuromorphic computing is an emerging research area that aims to build the next generation of artificial intelligence by taking inspiration from the brain [1]. One of the most significant advancements of this paradigm is the event camera [2], such as the Dynamic Vision Sensor (DVS) [3] and the Asynchronous Time-based Image Sensor (ATIS) [4]. Compared to the traditional cameras which output synchronous frames, the event cameras work in an asynchronous fashion and output events triggered

by the change of brightness, showing extremely high temporal resolution, low power consumption, and High Dynamic Range (HDR) imaging ability.

Events are formulated in Address-Event-Representation (AER). The  $i$ -th event in an event stream is  $E_i = (x_i, y_i, t_i, p_i)$ , where  $x_i, y_i$  are the coordinates,  $t_i$  is the timestamp and  $p_i$  is the polarity. The range of  $x_i, y_i$  is determined by the sensor’s spatial resolution, e.g.,  $0 \leq x_i \leq 127, 0 \leq y_i \leq 127$  for the DVS 128 camera. The temporal resolution of  $t_i$  is in  $\mu s$  range.  $p_i \in \{0, 1\}$  represents whether the brightness at position  $x_i, y_i$  is decreasing or increasing at timestamp  $t_i$ . The AER format is a sparse and irregular representation. However, most modern Computer Vision (CV) methods are based on dense and regular multi-dimensional tensor representation. For example, an image is represented as a tensor with the shape of  $C \times H \times W$ , where  $C$  is the number of channels,  $H$  is the height and  $W$  is the width. Typically,  $C = 1$  for grayscale image and  $C = 3$  for color image. The multi-dimensional tensor representation is compatible with deep learning methods [5], modern machine learning, and scientific computing frameworks [6–8].

To apply powerful deep learning methods in event-based vision, there are two successful solutions. The first category is a conversion method that converts events to dense and regular multi-dimensional tensor representations. Time surface [9], event-to-frame [10], and event-to-voxel [11] methods belong to the conversion category. After the conversion, dense and regular tensors are obtained and can be used by modern deep learning methods. However, these methods diminish and/or destroy temporal resolution of events since timestamps are quantized during conversion, and hence, conversion imposes large latency in real-time tasks [2, 12]. The second category is processing asynchronous and sparse events directly. Spiking neural networks (SNNs) [13, 14], sparse convolutional networks (sparse CNNs) [15], and graph neural networks (GNNs) [16, 17] are typical network structures that inherently possess sparse and asynchronous computations. However, modern deep learning methods rely heavily on Graphics Processing Units (GPUs), which are not well-suited for dynamic computations and unstructured sparse acceleration. Thus, these methods cannot fully utilize the massively parallel computational ability of GPUs and are much slower than traditional CNNs or dense models.

## 2 View of Encoding

Existing methods can also be regarded as solving the encoding problem of events, i.e., extracting and converting information from events to other formats. Conversion methods encode events to tensors with specific physical significances. For example, frames integrated from events are the sum of brightness changes during the temporal integration interval. SNNs encode events to spikes with spiking neurons. Sparse CNNs regard events as sparse images. GNNs take events as graphs, where, event-to-graph pre-processing is also required.

The most popular encoding method in machine learning is the word to vector (word2vec) [18], which solves the issue of representing words. It embeds each word to a fixed-length vector (token), and then the relationship between different words can be expressed by the math operations between vectors. This method is fully compatible

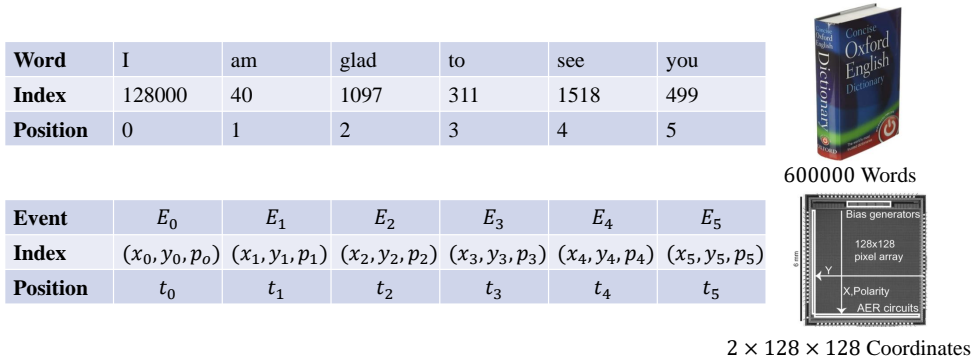


**Fig. 1:** Comparison between words and events. The figure of the DVS 128 camera is cited from [3].

with deep learning methods and has achieved significant success in Natural Language Processing (NLP) tasks [19, 20]. Another typical example is the Vision Transformer (ViT) [21], which yields significantly higher accuracy than CNNs owing to attention-based Transformer structure [22]. A vital component of ViT is the patchifying encoding method, which embeds image grids to tokens and enables Transformers to process images directly.

There are many similarities between words and events. Fig.1 shows the comparison between them. Our conclusions are as follows:

- (1) **Every element is a combination of an index and a position.** Each word has a unique index in the dictionary. Converting words to indices is implemented by the tokenizer in NLP tasks, and the indices in Fig.1 are generated by the Llama-3 [23] tokenizer. The position of a word is determined by the location in the sentence, e.g., 0 for "I" in the sentence "I am glad to see you". The index of an event is the tuple  $(x_i, y_i, p_i)$ . However, the position is not  $i$  but  $t_i$ , which indicates the temporal location in the event stream.
- (2) **The number of indices is finite.** A dictionary contains a certain number of words. An event camera can only output events with limited indices, e.g.,  $2 \times 128 \times 128$  for the DVS 128 camera, where 2 is the number of polarities and  $128 \times 128$  is the spatial resolution.
- (3) **The meaning of an element is determined by its context.** A word may have multiple meanings. For example, "transformer" means the neural network structure in deep learning, but can also represent roles in animated series. The meaning of a word is inferred by its context. An individual event indicates the brightness at a certain spatial and temporal location, but no more information can be inferred. However, a stream of events can form the outline of an object, then an event can be regarded as part of an edge. Thus, the meaning of an event is also determined by its context, the event stream.

### 3 Represent Event in Vector Space

Given the similarities between words and events, it is natural to represent events in vector space, i.e., event to vector (event2vec). For an event  $(x, y, t, p)$  obtained from an event camera with  $H \times W$  spatial resolution, we regard  $(x, y, p)$  as the spatial coordinate and  $t$  as the temporal position. We embed them to the embedding vector  $\mathbf{v} \in \mathbb{R}^d$ :

$$\mathbf{v} = \text{Embed}_s(x, y, p) + \text{Embed}_t(t), \quad (1)$$

where  $\text{Embed}_s(\cdot)$  is the spatial embedding module and  $\text{Embed}_t(\cdot)$  is the temporal encoding module. Eq.(1) fuses the spatial and temporal information by addition, which is also the most widely used fashion in LLMs.

#### 3.1 Spatial Embedding

A trivial formulation for the spatial embedding module is using the standard embedding layer for word2vec, which is implemented efficiently by a look-up-table:

$$\text{Embed}_s(x, y, p) = \mathbf{W}[p \cdot H \cdot W + y \cdot W + x], \quad (2)$$

where  $\mathbf{W} \in \mathbb{R}^{(2 \cdot H \cdot W) \times D}$  is the learnable embedding matrix and  $D$  is the embedding dimension. Eq.(2) maps each coordinate to a unique row index and selects the corresponding row from the embedding matrix.

The standard embedding layer does not preset any inductive bias between indices, and expects the model to learn relations between indices automatically. This design philosophy works well for words, for which the order of indices does not provide any information. For instance, we can not expect that the  $i$ -th word in a dictionary has a similar semantics to the  $(i + 1)$ -th word. However, it is not the case for event coordinates.

Since an image is a continuous two-dimensional function [24], it is widely known that pixels in a small neighborhood are similar. Thus, we expect that events with close coordinates should have similar semantics:

$$\text{Embed}_s(x + \Delta x, y + \Delta y, p + \Delta p) - \text{Embed}_s(x, y, p) \approx \mathbf{0}, \quad (3)$$

when  $[\Delta x, \Delta y, \Delta p] \approx \mathbf{0}$ .

However, Eq.(2) does not consider the neighbor semantics, which may cause difficulty for learning. To solve this issue, possible solutions include pre-training the embedding layer to learn neighborhood semantics, adding a neighborhood loss term, or using a weighted sum of neighbors centered by  $(x, y, p)$  as  $\text{Embed}_s(x, y, p)$ . Unfortunately, the former two methods require extra training procedures and parameter fine-tuning. The latter method causes computational costs to increase with the number of neighbors.

To achieve neighborhood semantics, we propose an elegant parametric algorithm 1 to generate the embedding matrix  $\mathbf{W}$ . As the algorithm 1 shows, we first generate

an arrangement  $\mathbf{c}$ , then convert it to the probe tensor  $[\mathbf{x}, \mathbf{y}, \mathbf{p}] \in \mathbb{N}^{(2 \cdot H \cdot W) \times 3}$ , which enumerates all event coordinates. Finally, we send the probe tensor to the parametric neural network  $\phi$ , and get the output embedding matrix  $\mathbf{W} \in \mathbb{R}^{(2 \cdot H \cdot W) \times D}$ .

---

**Algorithm 1** The parametric algorithm for generating the embedding matrix

---

**Require:** The height  $H$ , and width  $W$  of events; the parametric neural network  $\phi$

- 1:  $\mathbf{c} = [0, 1, \dots, P \cdot H \cdot W - 1]$
  - 2:  $\mathbf{x} = \mathbf{c} \bmod W$
  - 3:  $\mathbf{y} = \lceil \frac{\mathbf{c}}{W} \rceil \bmod H$
  - 4:  $\mathbf{p} = \lceil \frac{\mathbf{c}}{WH} \rceil$
  - 5:  $\mathbf{W} = \phi(\mathbf{x}, \mathbf{y}, \mathbf{p})$
- 

When using  $\mathbf{W}$  generated from the algorithm 1 in Eq.(2), for an arbitrary event coordinate  $(x, y, p)$ , it can be found that:

$$\mathbf{W}[p \cdot H \cdot W + y \cdot W + x] = \phi(x, y, p). \quad (4)$$

It is worth noting that  $\phi$  is continuous and differentiable. According to the Taylor series, we have:

$$\begin{aligned} & \phi(x + \Delta x, y + \Delta y, p + \Delta p) - \phi(x, y, p) = \\ & [\Delta x, \Delta y, \Delta p] \cdot \left[ \frac{\partial \phi}{\partial x}(x, y, p), \frac{\partial \phi}{\partial y}(x, y, p), \frac{\partial \phi}{\partial p}(x, y, p) \right]^T + o^n, \end{aligned} \quad (5)$$

where  $o^n$  represents the remainder term. Eq.(5) shows that when  $[\Delta x, \Delta y, \Delta p] \approx \mathbf{0}$ , then

$$\phi(x + \Delta x, y + \Delta y, p + \Delta p) - \phi(x, y, p) \approx \mathbf{0} + o^n \approx \mathbf{0}, \quad (6)$$

indicating that the embedding tensors of  $(x + \Delta x, y + \Delta y, p + \Delta p)$  and  $(x, y, p)$  are similar. Thus, we incorporate neighborhood semantics into the spatial embedding module by the parametric neural network  $\phi$ .

## 3.2 Temporal Encoding

Timestamps represent the occurrence time of events, whose role is similar to the indices of words in a sentence. Recently, relative positional encoding methods [25, 26] have attracted increasing interest and gradually substitute the absolute positional encoding method, such as the sinusoidal encoding [22] and the positional-wise learnable encoding [27].

However, applying relative positional encoding methods to timestamps is not reasonable. These encoding methods are designed for discrete and uniform indices, while timestamps are nearly continuous and uneven. To solve this issue, we employ a neural network to learn temporal encoding from the difference of timestamps.

More specifically, the temporal encoding is implemented by stacked convolutional layers, taking the one-order time difference  $t[i + 1] - t[i]$  for the  $i$ -th event in an event stream as inputs. Such a design brings the following advantages:

- (1) It utilizes the relative temporal distances of events directly, enabling the time-shift invariance.
- (2) It is a variant of position-wise learnable encoding but avoids the length generalization problem by taking continuous values as inputs.
- (3) The convolution operations involve adjacent events to generate the temporal encoding value of the center event, which is consistent with the neighborhood semantics.

## 4 Experiments

We validate the proposed event2vec methods on the neuromorphic DVS Gesture [28] and ASL-DVS [16] classification tasks. The DVS Gesture dataset contains 11 hand gesture categories and provides an official training/test split with 1176/288 samples. The ASL-DVS dataset contains 24 letters (classes) from the American Sign Language. Each class contains 4200 samples, and each sample lasts about 100 *ms*. We use the first 80% of the dataset as the training set and the last 20% as the test set. The train-test ratio is the same as [16]. To avoid any challenges with code reproducibility and allow fair comparison for researchers using our methodology, we do not split randomly.

### 4.1 Network Structure

We employ a multi-stage network structure to classify events, which is shown in Fig.2. The network contains the event2vec module, the linear attention backbone, and a linear layer as the final classification head.

#### 4.1.1 Event Embedding

As shown in Fig.2, the spatial embedding module  $\phi$  contains stacks of linear layers. It gradually increases the number of features from 3 to  $D$ . The layer normalization [29] layers are also inserted to stabilize training. Note that  $\phi$  generates the embedding matrix  $\mathbf{W}$  from the probe tensor as Algorithm 1, and then event coordinates are converted to tensors by Eq.(2). We can also use  $\phi$  to process event coordinates and get the same embedding tensors directly, as shown by Eq.(4). We can choose the indirect or the direct method flexibly according to their training speed.

The temporal encoding module has a similar structure to the spatial embedding module, except that it uses depth-wise convolutional layers with a kernel size of 3 and a stride of 1.

#### 4.1.2 Backbone

Eq.(1) embeds an event stream to a sequence, which can be processed by RNNs, Transformers, or temporal convolutional networks. The number of events in one event stream is also the length of tokens  $L$ , which is much longer than that of words in NLP

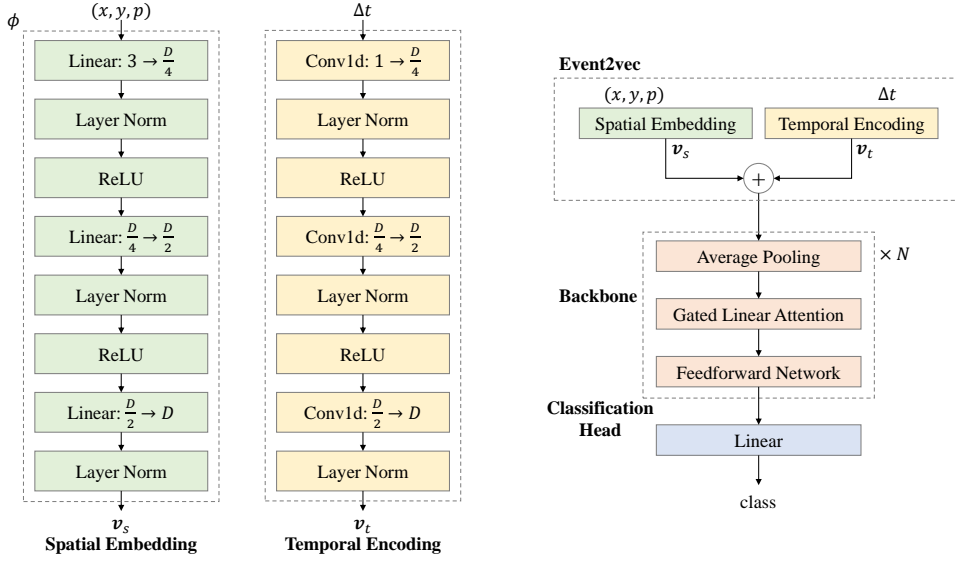


**Fig. 2:** The network structure for classifying event datasets with event2vec.

tasks. For example, the shortest sample in the DVS Gesture training dataset contains 35,267 events.

The space complexity of self-attention in Transformers is  $\mathcal{O}(L^2)$ , where  $L$  is the sequence length. Thus, it is impractical to process a long event stream with the vanilla Transformers. Fortunately, linear attentions [30–32] with the  $\mathcal{O}(L)$  space complexity have been proposed to solve the quadratic complexity problem. In this article, we employ the gated linear attention [33] to process event embedding tensors.

It is worth noting that linear attentions can also be regarded as RNNs [34]. To enhance the long-term learning ability of the gated linear attention for processing extremely long event streams, we extend it to a bi-directional formulation. Denote  $\mathbf{S}[t]$  as the hidden states at the time-step  $t$ , the recurrence of  $\mathbf{S}[t]$  in linear attentions obeys the following rule:

$$\mathbf{S}[t] = f(\mathbf{S}[t-1], \mathbf{k}[t], \mathbf{v}[t]), \quad (7)$$

where  $\mathbf{k}[t], \mathbf{v}[t]$  are input-dependent variables called as queries and keys, and  $f$  is specific for a certain linear attention. For example, the gated linear attention is:

$$\mathbf{S}[t] = \mathbf{G}[t] \odot \mathbf{S}[t-1] + \mathbf{v}[t]^T \mathbf{k}[t], \quad (8)$$

where  $G[t]$  is the input-dependent gate and  $\odot$  is the element-wise multiplication. We modify Eq.(7) as bi-directional, concatenate the forward directional  $\mathbf{S}_f[t]$  and backward direction  $\mathbf{S}_b[t]$ , and use a linear layer with weight  $\mathbf{W}_o$  to fuse them to generate

the final output  $\mathbf{O}[t]$ :

$$\mathbf{S}_f[t] = f(\mathbf{S}_f[t-1], \mathbf{k}[t], \mathbf{v}[t]), \quad (9)$$

$$\mathbf{S}_b[t] = f(\mathbf{S}_b[t-1], \mathbf{k}[L-t-1], \mathbf{v}[L-t-1]), \quad (10)$$

$$\mathbf{S}[t] = [\mathbf{S}_f[t], \mathbf{S}_b[t]], \quad (11)$$

$$\mathbf{O}[t] = \mathbf{W}_o \mathbf{S}[t]. \quad (12)$$

The structure of the backbone is shown in Fig.2, which contains  $N$  sequential linear attention blocks. Each block is composed of an average pooling layer, a gated linear attention, and a feedforward network with two linear layers and residual connections [35].

## 4.2 Event Sampling

The number of events in one sample is extremely large, and the lengths in different samples vary in a huge range, e.g., from 35,267 to 1,594,557 in the DVS Gesture training dataset. Neural networks process inputs in a batched computational fashion, which implies that tensors in one batch should have the identical shape. Thus, we sample  $L$  events from each event stream. When  $L$  is larger than the number of events in one stream, then it will be padded, and the padding mask will indicate to neural networks to ignore the padded events.

For each event stream in the DVS Gesture dataset, we randomly sample **without replacement** during training. Randomly sampling with replacement can hardly ensure that all events are sampled. For example, the average number of events in each sample in the DVS Gesture dataset is about 362,239. According to [36], if we randomly sample 4096 events from an event stream with 362,239 events, the expectation of sampling times to cover all events is about 900, indicating that randomly sampling with replacement is inefficient to utilize data. For the ASL-DVS dataset, we empirically find that randomly sampling with replacement works well, even if we have not traversed the whole training set. On the contrary, sampling without replacement requires a huge number of iterations to traverse the training set.

## 4.3 Training Hyper-parameters

We set all random seeds to 0. We use the AdamW [37] optimizer with the basic learning rate of 0.001, batch size 128, and cosine annealing learning rate scheduler [38]. The actual learning rate is scaled as

$$\text{learning\_rate} = \text{basic\_learning\_rate} \cdot \text{batch\_size} \cdot \text{world\_size}/256, \quad (13)$$

where  $\text{world\_size} = 4$  is the number of processes of distributed data parallel training. The specific hyperparameters for different datasets are as follows.

**DVS Gesture:** We set the embedding dim  $D = 128$ ; the convolutional kernel size 3 for the temporal encoding module; the key and value dims  $D_k = D_v = 64$ , the number of head  $n_{head} = 4$  for gated linear attentions;  $N = 8$  linear attention blocks in the backbone with pooling size in each block as 2, and the hidden feature  $D_{ffn} = 256$  for the

Dataset	Method	Preprocessing	Accuracy	Model Size (MB)	Used Training Data (%)
DVS Gesture	Sparse GRU [39]	To frame	97.80%	4.8	10,000
	SNN [40]	To frame	97.92%	0.13	19,200
	Ours	Randomly sampling 8192 events	96.01%	3.22	800
ASL-DVS	GNN+CNN [16]	To graph	90.10%	19.46	15,000
	GNN + Transformer [41]	To images and voxel-graph	99.60%	220.3	15,000
	Ours	Randomly sampling 512 events	99.80%	0.35	9.7

**Table 1:** Comparison of methods on DVS Gesture and ASL-DVS datasets.

feedforward network. The DVS Gesture dataset contains a small number of samples and is prone to causing overfitting, and we use a series of random data augmentations during training, including removing consecutive events, wrapping consecutive timestamps, resizing, rotation, shear transforming, and translation. We also set the weight decay to 2. The number of training epochs is 8. During training, we randomly sample 8192 events without replacement. During inference, we randomly sample 8192 events from each event stream. Due to the randomness of inference, we report the average test accuracy of repeating 18 times.

**ASL-DVS:** We set  $D = D_k = D_v = 64$ ,  $n_{head} = 2$ ,  $D_{ffn} = 128$ . The convolutional kernel size is 3 for the temporal encoding module. We only use  $N = 1$  linear attention block, and we set the pooling size in the block as 1 (no pooling). We do not use any data augmentation or weight decay. The number of epochs is 512. During training and inference, we randomly sample 512 events with replacement from each event stream, and the test accuracy is also reported by average over 16 repetitions.

#### 4.4 Analysis of Results

Tab.1 compares the results of our methods and some previous representative methods, where "Used Training Data (%)" is determined by both training epochs and event data preprocessing methods. For traditional preprocessing methods, such as event-to-frame and randomly sampling without replacement, the ratio is the number of training epochs. For randomly sampling with replacement, each event stream is only sampled once during one epoch. Thus, the ratio is approximately the number of sampled events over the number of events in the training set.

For the DVS Gesture dataset, our method achieves a sub-optimal accuracy compared to Sparse GRU [39] and SNN [40], which may be caused by the miniature scale of the dataset. For the ASL-DLV dataset, our method achieves slightly higher accuracy than previous methods, with a small model size and used training data ratio.

## 5 Discussion

The neuromorphic event cameras bring new opportunities and challenges for computer vision. Researchers have made massive efforts to bridge the gap between event-based vision and deep learning methods. In this article, we propose the first-of-its-kind

event2vec representation and enable neural networks to process asynchronous events directly without losing any temporal resolution.

The results on classifying DVS Gesture and ASL-DVS datasets validate the feasibility of processing events directly, and preprocessing methods such as event-to-frame can be avoided. At the same time, with only a few randomly sampled events, the model achieves comparable accuracy to previous methods, which take all events as inputs. Fewer events lead to less computational costs, memory consumption, latency, and energy demands, showing a promising prospect of deploying the model with event2vec on resource-limited edge computing devices. Although neuromorphic event cameras have  $\mu s$ -level temporal sensitivity, the computational speed of subsequent models cannot keep up with the preceding sensors in most cases. With the event2vec representation, the model gets rid of the latency of pre-processing the event data and has the potential to achieve  $ms$ -level response speed in an end-to-end scenario.

The most promising feature of event2vec is that it aligns events to the domain of natural language processing, which has achieved significant progress and attracted interest even outside academia and industry. By combining event2vec representation with powerful large language models, various applications can be explored. For example, we can use a decoder-only transformer structure and train on events with self-supervised learning, then the model is expected to generate future events from previous events like an "event-GPT". We can also build multi-modal large models incorporating events, images, and audio for low-latency and robust autonomous driving under complex environments. In conclusion, our research has the potential to extend the research topics of neuromorphic computing to generative tasks and applications.

## 6 Acknowledgment

This work was supported in part by CoCoSys, a JUMP2.0 center sponsored by DARPA and SRC, the National Science Foundation (CAREER Award, Grant #2312366, Grant #2318152), the DARPA Young Faculty Award and the DoE MMICC center SEA-CROGS (Award #DE-SC0023198).

## References

- [1] Mead, C.: Neuromorphic electronic systems. *Proceedings of the IEEE* **78**(10), 1629–1636 (1990) <https://doi.org/10.1109/5.58356>
- [2] Gallego, G., Delbrück, T., Orchard, G., Bartolozzi, C., Taba, B., Censi, A., Leutenegger, S., Davison, A.J., Conrath, J., Daniilidis, K., Scaramuzza, D.: Event-based vision: A survey. *IEEE Transactions on Pattern Analysis and Machine Intelligence* **44**(1), 154–180 (2022) <https://doi.org/10.1109/TPAMI.2020.3008413>
- [3] Lichtsteiner, P., Posch, C., Delbruck, T.: A  $128 \times 128$  120 db 15  $\mu s$  latency asynchronous temporal contrast vision sensor. *IEEE Journal of Solid-State Circuits* **43**(2), 566–576 (2008) <https://doi.org/10.1109/JSSC.2007.914337>

- [4] Posch, C., Matolin, D., Wohlgenannt, R.: A qvga 143 db dynamic range frame-free pwm image sensor with lossless pixel-level video compression and time-domain cds. *IEEE Journal of Solid-State Circuits* **46**(1), 259–275 (2011) <https://doi.org/10.1109/JSSC.2010.2085952>
- [5] LeCun, Y., Bengio, Y., Hinton, G.: Deep learning. *Nature* **521**(7553), 436–444 (2015) <https://doi.org/10.1038/nature14539>
- [6] Abadi, M., Barham, P., Chen, J., Chen, Z., Davis, A., Dean, J., Devin, M., Ghemawat, S., Irving, G., Isard, M., Kudlur, M., Levenberg, J., Monga, R., Moore, S., Murray, D.G., Steiner, B., Tucker, P., Vasudevan, V., Warden, P., Wicke, M., Yu, Y., Zheng, X.: Tensorflow: a system for large-scale machine learning. In: *Proceedings of the 12th USENIX Conference on Operating Systems Design and Implementation. OSDI'16*, pp. 265–283. USENIX Association, USA (2016)
- [7] Paszke, A., Gross, S., Massa, F., Lerer, A., Bradbury, J., Chanan, G., Killeen, T., Lin, Z., Gimelshein, N., Antiga, L., Desmaison, A., Kopf, A., Yang, E., DeVito, Z., Raison, M., Tejani, A., Chilamkurthy, S., Steiner, B., Fang, L., Bai, J., Chintala, S.: Pytorch: An imperative style, high-performance deep learning library. In: Wallach, H., Larochelle, H., Beygelzimer, A., Alché-Buc, F., Fox, E., Garnett, R. (eds.) *Advances in Neural Information Processing Systems*, vol. 32 (2019)
- [8] Harris, C.R., Millman, K.J., Walt, S.J., Gommers, R., Virtanen, P., Cournapeau, D., Wieser, E., Taylor, J., Berg, S., Smith, N.J., Kern, R., Picus, M., Hoyer, S., Kerkwijk, M.H., Brett, M., Haldane, A., Río, J.F., Wiebe, M., Peterson, P., Gérard-Marchant, P., Sheppard, K., Reddy, T., Weckesser, W., Abbasi, H., Gohlke, C., Oliphant, T.E.: Array programming with numpy. *Nature* **585**(7825), 357–362 (2020) <https://doi.org/10.1038/s41586-020-2649-2>
- [9] Lagorce, X., Orchard, G., Galluppi, F., Shi, B.E., Benosman, R.B.: Hots: A hierarchy of event-based time-surfaces for pattern recognition. *IEEE Transactions on Pattern Analysis and Machine Intelligence* **39**(7), 1346–1359 (2017) <https://doi.org/10.1109/TPAMI.2016.2574707>
- [10] Liu, M., Delbruck, T.: Adaptive time-slice block-matching optical flow algorithm for dynamic vision sensors. (2018). *BMVC*
- [11] Bardow, P., Davison, A.J., Leutenegger, S.: Simultaneous optical flow and intensity estimation from an event camera. In: *Proceedings of the IEEE Conference on Computer Vision and Pattern Recognition (CVPR)* (2016)
- [12] Rebecq, H., Ranftl, R., Koltun, V., Scaramuzza, D.: Events-to-video: Bringing modern computer vision to event cameras. In: *Proceedings of the IEEE/CVF Conference on Computer Vision and Pattern Recognition*, pp. 3857–3866 (2019)
- [13] Maass, W.: Networks of spiking neurons: the third generation of neural network models. *Neural networks* **10**(9), 1659–1671 (1997)

- [14] Roy, K., Jaiswal, A., Panda, P.: Towards spike-based machine intelligence with neuromorphic computing. *Nature* **575**(7784), 607–617 (2019)
- [15] Messikommer, N., Gehrig, D., Loquercio, A., Scaramuzza, D.: Event-based asynchronous sparse convolutional networks. (2020)
- [16] Bi, Y., Chadha, A., Abbas, A., Bourtsoulatze, E., Andreopoulos, Y.: Graph-based object classification for neuromorphic vision sensing. In: 2019 IEEE/CVF International Conference on Computer Vision (ICCV), pp. 491–501 (2019). <https://doi.org/10.1109/ICCV.2019.00058>
- [17] Schaefer, S., Gehrig, D., Scaramuzza, D.: Aegnn: Asynchronous event-based graph neural networks. In: 2022 IEEE/CVF Conference on Computer Vision and Pattern Recognition (CVPR), pp. 12361–12371 (2022). <https://doi.org/10.1109/CVPR52688.2022.01205>
- [18] Mikolov, T., Sutskever, I., Chen, K., Corrado, G.S., Dean, J.: Distributed representations of words and phrases and their compositionality. In: Burges, C.J., Bottou, L., Welling, M., Ghahramani, Z., Weinberger, K.Q. (eds.) *Advances in Neural Information Processing Systems*, vol. 26. Curran Associates, Inc., Lake Tahoe, Nevada, USA (2013)
- [19] Devlin, J., Chang, M.-W., Lee, K., Toutanova, K.: BERT: Pre-training of deep bidirectional transformers for language understanding. In: Burstein, J., Doran, C., Solorio, T. (eds.) *Proceedings of the 2019 Conference of the North American Chapter of the Association for Computational Linguistics: Human Language Technologies, Volume 1 (Long and Short Papers)*, pp. 4171–4186. Association for Computational Linguistics, Minneapolis, Minnesota (2019). <https://doi.org/10.18653/v1/N19-1423>
- [20] Brown, T., Mann, B., Ryder, N., Subbiah, M., Kaplan, J.D., Dhariwal, P., Neelakantan, A., Shyam, P., Sastry, G., Askell, A., Agarwal, S., Herbert-Voss, A., Krueger, G., Henighan, T., Child, R., Ramesh, A., Ziegler, D., Wu, J., Winter, C., Hesse, C., Chen, M., Sigler, E., Litwin, M., Gray, S., Chess, B., Clark, J., Berner, C., McCandlish, S., Radford, A., Sutskever, I., Amodei, D.: Language models are few-shot learners. In: *Advances in Neural Information Processing Systems*, vol. 33, pp. 1877–1901. Curran Associates, Inc., Virtual (2020)
- [21] Dosovitskiy, A., Beyer, L., Kolesnikov, A., Weissenborn, D., Zhai, X., Unterthiner, T., Dehghani, M., Minderer, M., Heigold, G., Gelly, S., Uszkoreit, J., Houlsby, N.: An image is worth 16x16 words: Transformers for image recognition at scale. In: *International Conference on Learning Representations* (2021)
- [22] Vaswani, A., Shazeer, N., Parmar, N., Uszkoreit, J., Jones, L., Gomez, A.N., Kaiser, L.u., Polosukhin, I.: Attention is all you need. In: Guyon, I., Luxburg, U.V., Bengio, S., Wallach, H., Fergus, R., Vishwanathan, S., Garnett, R. (eds.) *Advances in Neural Information Processing Systems*, vol. 30. Curran Associates,

- Inc., Long Beach, California, USA (2017)
- [23] Grattafiori, A., Dubey, A., Jauhri, A., Pandey, A., Kadian, A., Al-Dahle, A., Letman, A., Mathur, A., Schelten, A., Vaughan, A., et al.: The llama 3 herd of models. arXiv preprint arXiv:2407.21783 (2024)
- [24] Gonzalez, R.C.: Digital Image Processing. Pearson education india, India (2009)
- [25] Press, O., Smith, N.A., Lewis, M.: Train short, test long: Attention with linear biases enables input length extrapolation. arXiv preprint arXiv:2108.12409 (2021)
- [26] Su, J., Ahmed, M., Lu, Y., Pan, S., Bo, W., Liu, Y.: Roformer: Enhanced transformer with rotary position embedding. *Neurocomputing* **568**, 127063 (2024)
- [27] Devlin, J., Chang, M.-W., Lee, K., Toutanova, K.: Bert: Pre-training of deep bidirectional transformers for language understanding. In: Proceedings of the 2019 Conference of the North American Chapter of the Association for Computational Linguistics: Human Language Technologies, Volume 1 (long and Short Papers), pp. 4171–4186 (2019)
- [28] Amir, A., Taba, B., Berg, D., Melano, T., McKinstry, J., Di Nolfo, C., Nayak, T., Andreopoulos, A., Garreau, G., Mendoza, M., Kusnitz, J., Debole, M., Esser, S., Delbruck, T., Flickner, M., Modha, D.: A low power, fully event-based gesture recognition system. In: 2017 IEEE Conference on Computer Vision and Pattern Recognition (CVPR), pp. 7388–7397 (2017). <https://doi.org/10.1109/CVPR.2017.781>
- [29] Ba, J.L., Kiros, J.R., Hinton, G.E.: Layer normalization. arXiv preprint arXiv:1607.06450 (2016)
- [30] Sun, Y., Dong, L., Huang, S., Ma, S., Xia, Y., Xue, J., Wang, J., Wei, F.: Retentive network: A successor to transformer for large language models. arXiv preprint arXiv:2307.08621 (2023)
- [31] Gu, A., Dao, T.: Mamba: Linear-time sequence modeling with selective state spaces. In: First Conference on Language Modeling (2024)
- [32] Peng, B., Alcaide, E., Anthony, Q., Albalak, A., Arcadinho, S., Biderman, S., Cao, H., Cheng, X., Chung, M., Derczynski, L., Du, X., Grella, M., Gv, K., He, X., Hou, H., Kazienko, P., Kocon, J., Kong, J., Koptyra, B., Lau, H., Lin, J., Mantri, K.S.I., Mom, F., Saito, A., Song, G., Tang, X., Wind, J., Woźniak, S., Zhang, Z., Zhou, Q., Zhu, J., Zhu, R.-J.: RWKV: Reinventing RNNs for the transformer era. In: Bouamor, H., Pino, J., Bali, K. (eds.) Findings of the Association for Computational Linguistics: EMNLP 2023, pp. 14048–14077. Association for Computational Linguistics, Singapore (2023). <https://doi.org/10.18653/v1/2023>.

- [33] Yang, S., Wang, B., Shen, Y., Panda, R., Kim, Y.: Gated linear attention transformers with hardware-efficient training. In: Salakhutdinov, R., Kolter, Z., Heller, K., Weller, A., Oliver, N., Scarlett, J., Berkenkamp, F. (eds.) Proceedings of the 41st International Conference on Machine Learning. Proceedings of Machine Learning Research, vol. 235, pp. 56501–56523. PMLR, Seoul, South Korea (2024)
- [34] Katharopoulos, A., Vyas, A., Pappas, N., Fleuret, F.: Transformers are RNNs: Fast autoregressive transformers with linear attention. In: III, H.D., Singh, A. (eds.) Proceedings of the 37th International Conference on Machine Learning. Proceedings of Machine Learning Research, vol. 119, pp. 5156–5165. PMLR, Virtual (2020)
- [35] He, K., Zhang, X., Ren, S., Sun, J.: Deep residual learning for image recognition. In: Proceedings of the IEEE Conference on Computer Vision and Pattern Recognition, pp. 770–778 (2016)
- [36] Stadje, W.: The collector’s problem with group drawings. *Advances in Applied Probability* **22**(4), 866–882 (1990)
- [37] Loshchilov, I., Hutter, F.: Decoupled weight decay regularization. In: International Conference on Learning Representations (2019)
- [38] Loshchilov, I., Hutter, F.: SGDR: Stochastic gradient descent with warm restarts. In: International Conference on Learning Representations (2017)
- [39] Subramoney, A., Nazeer, K.K., Schöne, M., Mayr, C., Kappel, D.: Efficient recurrent architectures through activity sparsity and sparse back-propagation through time. In: The Eleventh International Conference on Learning Representations (2023)
- [40] Fang, W., Yu, Z., Chen, Y., Huang, T., Masquelier, T., Tian, Y.: Deep residual learning in spiking neural networks. *Advances in Neural Information Processing Systems* **34**, 21056–21069 (2021)
- [41] Yuan, C., Jin, Y., Wu, Z., Wei, F., Wang, Y., Chen, L., Wang, X.: Learning bottleneck transformer for event image-voxel feature fusion based classification. In: Chinese Conference on Pattern Recognition and Computer Vision (PRCV), pp. 3–15 (2023). Springer